

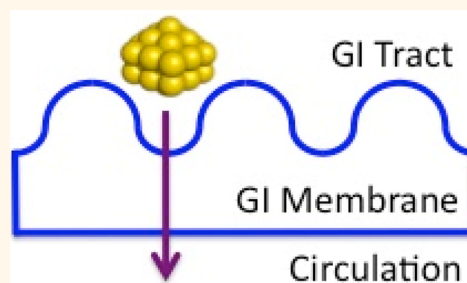
Gastrointestinal Bioavailability of 2.0 nm Diameter Gold Nanoparticles

Candice A. Smith, Carrie A. Simpson, Ganghyeok Kim, Carly J. Carter, and Daniel L. Feldheim*

Department of Chemistry and Biochemistry, University of Colorado, Boulder, Colorado 80309, United States

ABSTRACT The use of gold nanoparticles as imaging agents and therapeutic delivery systems is growing rapidly. However, a significant limitation of gold nanoparticles currently is their low absorption efficiencies in the gastrointestinal (GI) tract following oral administration. In an attempt to identify ligands that facilitate gold nanoparticle absorption in the GI tract, we have studied the oral bioavailability of 2.0 nm diameter gold nanoparticles modified with the small molecules *p*-mercaptobenzoic acid and glutathione, and polyethylene glycols (PEG) of different lengths and charge (neutral and anionic). We show that GI absorption of gold nanoparticles modified with the small molecules tested was undetectable. However, the absorption of PEGs depended upon PEG

length, with the shortest PEG studied yielding gold nanoparticle absorptions that are orders-of-magnitude larger than observed previously. As the oral route is the most convenient one for administering drugs and diagnostic reagents, these results suggest that short-chain PEGs may be useful in the design of gold nanoparticles for the diagnosis and treatment of disease.



KEYWORDS: gold nanoparticles · oral bioavailability · gastrointestinal absorption

Nanometer-sized gold particles, including nanoclusters, nanorods, and nanoshells, are quickly becoming valuable tools to study, diagnose, and treat disease. With light extinctions that are remarkably large (10^6 – 10^9 M^{-1} cm^{-1}) and tunable across the visible–near-infrared spectrum, gold nanoparticles are being used to detect nucleic acids and proteins inside of live cells and from blood plasma with unprecedented limits of detection^{1–3} and to treat a variety of cancers *via* mechanisms such as laser-induced thermal ablation.^{4–9} The ease with which gold nanoparticles can be functionalized with a mixed monolayer of small molecules, polymers, proteins, and DNA has also made them attractive platforms for the assembly of multifunctional drug delivery systems that are capable of specific cell and nuclear targeting and even transdermal delivery.^{10–14}

Our lab has developed a highly combinatorial therapeutic discovery method based upon 2.0 nm diameter organothiol-modified gold nanoparticles.^{15,16} This method exploits the ease with which several chemically distinct organothiol ligands may be attached covalently to a single gold nanoparticle. By screening libraries of mixed thiol

monolayer–gold nanoparticle conjugates we have been able to identify nanoparticles with potent bacterial growth inhibition activities against several strains of the Gram-negative bacteria *E. coli* and *K. pneumoniae*.

These results have motivated us to explore the potential for developing gold nanoparticle antibiotics that are administered orally. The oral bioavailability of gold nanoparticles has been examined only to a limited extent previously. Albrecht added citrate-coated gold nanoparticles with diameters of 4, 10, 28, and 58 nm to drinking water for administration to mice *ad libitum*.¹⁷ With the exception of the largest nanoparticles, all particles were found in the major organs at levels on the order of ones to tens of ng Au/g of tissue. The bioavailability of the nanoparticles as a percentage of the dose administered could not be calculated because the amount ingested was unknown. Schleh administered sulfonated triphenylphosphine- and thiol-modified gold nanoparticles from 1.8 to 200 nm in diameter to rats *via* oral gavage.¹⁸ Positively and negatively charged thiols were examined, and >99.63% of the particles administered were found either in the gastrointestinal (GI) tract

* Address correspondence to Daniel.Feldheim@Colorado.edu.

Received for review December 21, 2012 and accepted April 21, 2013.

Published online April 21, 2013
10.1021/nn305930e

© 2013 American Chemical Society

or feces regardless of size and charge. The conclusion from these studies is that gold nanoparticles are not absorbed in the GI tract to a large extent in both an absolute sense and relative to most small-molecule antibiotics.

In an attempt to identify molecular monolayers that might increase the absorption of gold nanoparticles in the GI tract, we have studied the oral bioavailability of 2.0 nm diameter gold nanoparticles modified with the small molecules *p*-mercaptobenzoic acid (pMBA) and glutathione (GSH), and polyethyleneglycols (PEG) of different lengths (4, 12, and 24 EG units) and charge (neutral and anionic). PEGs were chosen because they have been shown to be absorbed in large quantities, up to 60% for PEG4.¹⁹ Here we show that GI absorption of gold nanoparticles modified with the small molecules tested was undetectable. However, the absorption of PEGs depended upon PEG length, with the smallest PEG studied yielding unprecedented gold nanoparticle GI absorption efficiencies.

RESULTS AND DISCUSSION

In order to be absorbed in the GI tract and circulate systemically, a nanoparticle must be able to avoid aggregation and chemical degradation as it travels through the stomach and into the intestines. Perhaps the most formidable challenge to nanoparticle stability along this route is pH. The pH in the mouse GI tract can be as low as 3 in the stomach and as high as 5 in the intestines. In humans the pH in the stomach and intestines is approximately 2 and 8, respectively. These conditions could alter ligand charge or cause ligand displacement that changes the physicochemical properties of the nanoparticle or leads to particle aggregation.

To measure the stability of our nanoparticles in solutions with a pH of 2 and 8, glutathione-coated gold nanoparticles were synthesized and subjected to ligand exchange reactions to generate PEG-modified gold nanoparticle conjugates. The gold nanoparticle conjugates were analyzed by NMR to qualitatively confirm ligand exchange and by TEM to measure particle diameter (Figures S1–S8, Supporting Information). NMR showed that all PEGs studied were able to displace glutathione and bind to the nanoparticles. NMR also suggested that the exchange yield was high, as glutathione was not detected following ligand exchange and nanoparticle purification. The nanoparticle solutions were then adjusted to pH 2 and warmed to 37 °C for 2 h. During this time, the plasmon extinction band of the gold nanoparticles was monitored by UV–visible spectroscopy to assess the stability of the nanoparticle conjugates (Figure S10). After 2 h, the pH was adjusted to 8 and the solutions were monitored for an additional 4 h. No significant spectral changes were observed for the PEG conjugates over the entire pH and time range studied. A slight drop in the plasmon absorption band was observed for the pMBA-modified gold

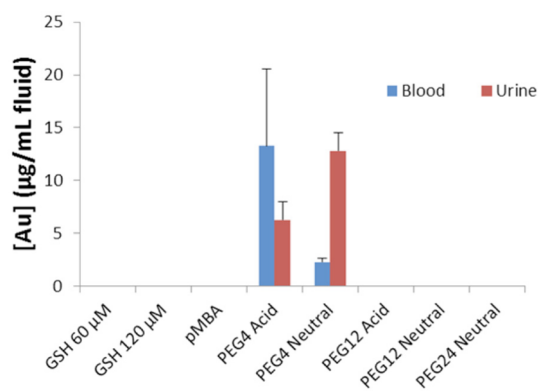


Figure 1. Gold accumulation in blood and urine over a 24 h period. Samples were collected at 1, 8, and 24 h, and the gold concentrations measured at each time point summed to generate the bars shown. Gold concentrations were undetectable in all administrations except for the PEG4 ligands.

nanoparticles at pH 2 over the course of 2 h, which likely indicates slight precipitation due to pMBA protonation. In contrast, the plasmon band of glutathione-modified gold nanoparticles appeared to sharpen over time at pH 2, which suggests that some size focusing (Ostwald ripening) may occur.

Given their stability under conditions of pH that includes those found in the mouse GI tract, pMBA-Au, glutathione-Au, and all of the PEG conjugates were advanced to oral bioavailability studies. Glutathione-coated gold nanoparticles have been shown to be nontoxic by subcutaneous injection up to and including 60 µM.²⁰ Given this prior observation, 60 µM concentrations were used for all initial gavage experiments (200 µL administrations). An additional experiment was conducted on glutathione particles at 120 µM. Blood, urine, organs (heart, liver, lungs, spleen, kidney, stomach, and intestines), and feces were examined for gold content using ICP-MS. Urine was collected at three time points, 1 h, 8 h, and 24 h, as described previously.²⁰ These values were then added (error propagated) to produce a renal output value over the entire 24 h period.

For the small-molecule adsorbates glutathione and pMBA, no gold was detected in the urine, blood, or any of the organs tested (Figures 1 and 2). Doubling the concentration of glutathione-coated gold nanoparticles did not result in a detectable amount of gold in the blood or urine. This is not surprising, as large quantities of glutathione alone (up to 3 g) administered orally do not cross the GI tract in appreciable amounts.²¹

The addition of PEG to the nanoparticles had a profound effect on GI absorption. The most surprising discovery was the high concentrations of gold detected in the blood and urine following oral administration of both the acid and neutral forms of the PEG4-modified nanoparticles (Figure 1). Detectable levels of gold were also discovered in both major filtration organs (liver and kidneys; Figure 2), confirming gold

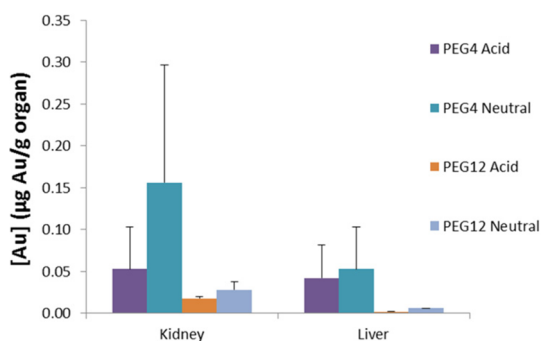


Figure 2. Gold distribution in the kidneys and liver for gold nanoparticles administered orally. Detectable concentrations of gold were noted for PEG₄- and PEG₁₂-modified particles, indicating absorption in the GI tract. PEG₄ had the highest accumulation of all formulations, indicating PEG length may be responsible for gastrointestinal absorbance. No gold was detected for the other modified nanoparticles.

absorption followed by systemic circulation and organ targeting. TEM of urine samples collected following oral administration of the neutral PEG₄-modified nanoparticles revealed particles with diameters of 2.3 ± 0.7 nm (Figure S11). As these nanoparticles are similar in size to PEG₄-Au nanoparticles prior to administration 1.9 ± 0.4 nm (Figure S9), we presume that the source of gold in the blood, urine, and organs was gold nanoparticles that traveled through the GI tract and circulatory system intact. Together the ICP-MS and TEM data suggest that PEG₄ dramatically increased the oral bioavailability of gold nanoparticles compared to what is afforded by small-molecule ligands such as pMBA, glutathione, or citrate. It was then of interest to determine if longer PEG chains could provide even larger GI absorption efficiencies.

In contrast to the PEG₄-modified nanoparticles, gold was not detected in the blood, urine, or tissues for nanoparticles modified with either the neutral or carboxylate forms of PEG₁₂ (Figure 1 and 2). Gold was also undetectable in the blood and urine for the PEG₂₄ conjugate (Figure 1). However, a relatively small quantity of gold was found in the liver and kidneys for the PEG₁₂ conjugates (Figure 2), which suggests that they were absorbed in the GI tract, circulated systemically, and concentrated in the filter organs. Thus, while there was no noticeable dependence of GI absorption upon PEG charge, there appears to be a dependence upon PEG length, with shorter chain PEGs providing increased GI absorption.

Final consideration of the fate of these gold nanoparticles following oral administration was focused on the components of the GI tract itself—the stomach, intestines, and excreted feces (Figure 3). Feces were collected in the same manner and at the same time points as blood and urine, and their values summed for comprehensive analysis over a 24 h period. Stomach and intestines were removed at the same time as the other organs, 24 h postadministration. The data show

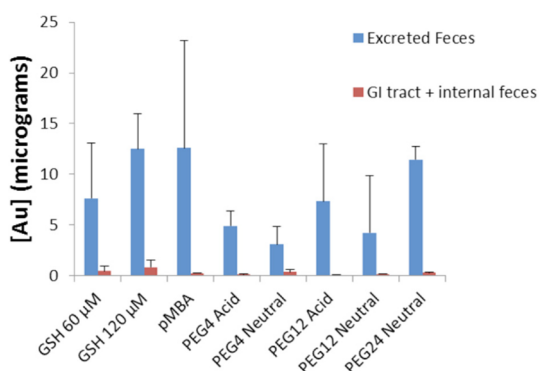


Figure 3. Fecal and gastrointestinal distribution of gold nanoparticles. Samples were collected at 1, 8, and 24 h, and the gold concentrations measured at each time point summed to generate the bars shown. Nanoparticle concentrations were $60 \mu\text{M}$ except where indicated.

that gold was present in the GI tract and excreted feces following administration of all of the nanoparticles. An increase in fecal gold mass with an increase in the concentration of glutathione-Au nanoparticles administered was noted, indicating that input and output are correlative. In addition, the mass of gold detected in feces for nanoparticles modified with PEG₂₄ was higher than its PEG₄ counterparts (Student's *t* test, 95% confidence interval), which is consistent with their relative absorption efficiencies. No statistical difference was noted between the acid and neutral end groups with regard to excretion in fecal material.

The goal of this study was to begin to elucidate some basic design principles for the assembly of 2.0 nm diameter ligand-modified gold nanoparticles with increased oral bioavailability. Two small molecules were examined as ligands, the zwitterionic glutathione and the anionic pMBA. Gold conjugates modified with these ligands were not detected in blood, urine, or any of the organs examined. Monolayers containing PEG, however, increased nanoparticle absorption in the GI tract dramatically, with the shorter PEGs providing increased absorption efficiencies. This trend could be a function of hydrodynamic radius, as larger particles have been shown to hinder the absorption process.^{17,18} However, this same trend has been noted even for free PEGs;¹⁹ an increase in PEG molecular weight from 600 to 1000 Da produced a decrease in absorption from 60% to 9%. The PEG₄ ligands used in our study have molecular weights of 395 or 454 Da, close to the free PEG with the best absorption efficiency.

Although the mass of gold detected in the blood and urine following administration of PEG₄-Au nanoparticles was similar for the neutral and carboxylic acid PEGs, there was a difference in how the two types of nanoparticles were distributed. The PEG₄-neutral nanoparticles appeared to be cleared *via* the renal system more rapidly, as they were found predominantly in the urine *versus* the blood after 24 h. In contrast, the PEG₄-acid particles were found in a larger proportion in the

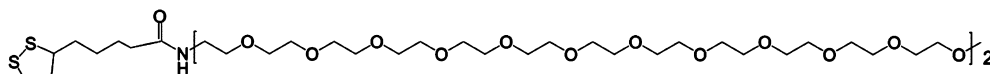
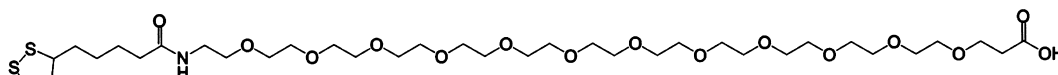
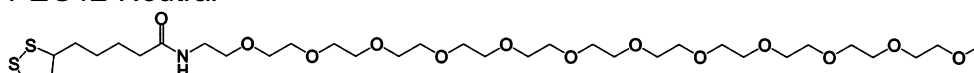
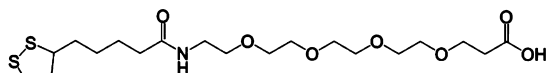
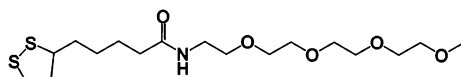
PEG24-Neutral**PEG12-Acid****PEG12-Neutral****PEG4-Acid****PEG4-Neutral**

Figure 4. Structural illustrations of cyclic disulfide-terminated polyethylene glycol ligands.

blood *versus* the urine in 24 h. This is consistent with previous reports on gold nanoparticles modified with carboxylic acid and neutral PEGs, which showed longer circulation lifetimes for acid-terminated PEG-modified gold nanoparticles administered *via* subcutaneous injection.²²

Finally, although we cannot accurately calculate the percentage of gold nanoparticles that were absorbed in the GI tract because we did not collect all of the urine excreted over the entire 24 h time course, we can place a lower limit on the absorption efficiency. For the PEG4-acid, the mass of gold detected in the urine, blood, and organs was on average 18 μg and the total mass administered was 360 μg . The minimum average amount absorbed into the systemic circulation was thus $\sim 5\%$. This is several orders-of-magnitude larger than reported in previous studies.

CONCLUSIONS

The ease with which gold nanoparticles may be synthesized and modified with a plurality of ligands makes them attractive candidates as imaging agents, therapeutics, and therapeutic delivery systems. The most attractive route for administering drugs and diagnostic agents is orally. The ability to modify gold nanoparticles to facilitate their gastrointestinal absorption could create new opportunities in medicine, particularly

for diseases that require frequent administrations and prolonged treatments, and in regions of the world where other forms of administration are impractical and engender a significant health risk (*e.g.*, intravenous injection). The gold nanoparticle antibiotics discovered in our lab are one example where oral bioavailability will be important if a translation to the clinic is to be made. It is interesting to consider further the possibility that therapeutically viable drugs that have been shelved due to poor oral bioavailability might be rescued *via* conjugation to PEG4-modified gold nanoparticles. It is equally important to not overlook the observation that certain PEGs and small molecules can prevent nanoparticle absorption in the GI tract. Many important disease targets exist in the small and large intestines, and confining a drug to the GI tract can lower the therapeutic drug dose required and prevent side effects that occur upon systemic circulation. Although we have yet to investigate whether PEG4 can be combined onto gold with other small molecules without compromising GI absorption efficiency, the results presented here suggest that 2.0 nm diameter gold nanoparticles containing PEG4 may be a useful platform for the synthesis of orally bioavailable nanoparticle therapeutics, while nanoparticles modified with pMBA, glutathione, or PEG24 may be suitable for therapeutics designed for intestinal targets.

EXPERIMENTAL METHODS

Synthesis of Gold Nanoparticles. Glutathione-coated gold nanoparticles and pMBA-coated gold nanoparticles were synthesized according to our previous publications.^{16,20} A solution of 20 mM HAuCl_4 (Strem, Newburyport, MA, USA) dissolved in 20 mL of methanol was combined with either 16 mL of 85.0 mM glutathione in ultrapure water (Sigma Aldrich, St. Louis, MO,

USA) or 85.0 mM pMBA dissolved in pH 12 ultrapure water. Gold mixtures were allowed to equilibrate for 15 min while stirring. The solutions (0.40 mmol of Au^{3+}) were diluted to a final Au^{3+} concentration of 0.55 mM with the addition of 202 mL of ultrapure water and 186 mL of methanol. The Au^{3+} was reduced with 7.2 mL of a 0.25 mM aqueous sodium borohydride (Sigma Aldrich) solution. The reduction was allowed to proceed for 24 h at room temperature with constant stirring. Gold nanoparticles

were precipitated with the addition of 120 mmol of NaCl in 720 mL of methanol followed by centrifugation at 3200 RCF for 5 min. Precipitated nanoparticles were reconstituted in water. The concentration was measured by UV–visible spectroscopy using the extinction coefficient of $400\,000\text{ M}^{-1}\text{ cm}^{-1}$ at 510 nm. The diameter of the pMBA-Au nanoparticles was 1.7 ± 0.40 nm, as determined by transmission electron microscopy. This size is similar to pMBA-Au nanoparticles characterized by X-ray crystallography to have a molecular formula of $\text{Au}_{144}(\text{pMBA})_{60}$.²³ The diameter of the glutathione-Au nanoparticles was 2.0 ± 0.60 nm.

Place-Exchange of Polyethylene Glycols onto Glutathione-Coated Gold Nanoparticles. Stock solutions of the cyclic disulfide-terminated polyethylene glycols, from Quanta Biodesign, were prepared in either water (PEG4-neutral and PEG24-neutral) or dimethyl sulfoxide (PEG4-acid, PEG12-neutral, and PEG12-acid). To a 10 μM solution of glutathione-coated gold nanoparticles in Milli-Q water (18 m Ω) was added an aliquot of PEG stock solution to a final concentration of 1 mM. Exchange was replicated in 20 individual tubes each with a total volume of 4 mL. Solutions were placed on a shaker at 19 °C and allowed to mix for 24 h. Particles were precipitated by adding 2 mL of a 4 M NaCl solution followed by centrifugation at 3200 RCF for 15 min. Precipitated particles were allowed to air-dry for 24 h. Particles were then suspended in water, and all 20 tubes were combined and washed three times over a 30K MWCO amicon filter. The final concentration was determined by UV–visible spectroscopy as described above.

Nuclear Magnetic Resonance Spectroscopy. NMR was used to assess the extent of ligand substitution. The gold nanoparticle samples were analyzed by ¹H NMR on a 500 MHz Varian Inova spectrometer in a solution of deuterium oxide/water with a water suppression program. For comparison, pure ligands were suspended in a mixture of deuterium oxide/water for all PEG and small molecules except for PEG12N, which was in a mixture of 90% D₂O/10% DMSO. A gradient COSY was run on both the glutathione ligand and glutathione-coated nanoparticle to show correlative cross-peaks of *J*-coupled signals. All spectra can be found within the Supporting Information, Figures S1–S8.

Transmission Electron Microscopy (TEM). TEM grids were prepared by placing a drop of the gold nanoparticles on a carbon film-covered copper mesh grid for a minute, and then excess solution was wicked away with a paper filter. Grids were then allowed to air-dry for 45 min before being imaged by TEM. The subsequent TEM images were analyzed by Image-J to determine the size distribution of the gold nanoparticle cores. A minimum of 100 particles was measured before analysis of size distribution.

Samples of urine were concentrated with 30 kDa MWCO Amicon filters and washed three times with 400 μL volumes of Milli-Q water. Then 5 μL of the resultant sample was applied to a copper grid, and the excess solution wicked away. Due to excess salt, the grids were rinsed twice with ultrapure water, by applying 10 μL of Milli-Q water, wicking the solution away, and allowing the grid to dry.

Animal Models. Animals were housed at the Keck Facility, a University of Colorado Division of Animal Care (DAC) facility, fully certified by the Association for Assessment and Accreditation of Laboratory Animal Care (AAALAC). Animals were housed under the full supervision of the full-time veterinarian and staff. All procedures performed were previously approved by the University of Colorado's Institutional Animal Care and Use Committee (IACUC). Balb/c, 5–6-week-old, 15–16 g, female mice were purchased from Harlan Laboratories. Nanoparticle formulations were prepared in Milli-Q water ($n = 5$ mice per formulation). Plastic oral gavage needles (20 gauge, 3.8 mm length) were purchased from Instech Soloman. A 60 or 120 μM concentration in a 200 μL volume of each nanoparticle formulation was administered to five individual mice by oral gavage (45 mice total). Blood was drawn *via* submandibular bleeding techniques,²⁴ in compliance with our protocol and bleeding guidelines for mL/kg body weight per week.²⁵ Urine was collected on cellophane with precautions taken to avoid fecal contamination.²⁶ Feces were also collected separately on cellophane. Mice were euthanized at 24 h by carbon dioxide

asphyxiation followed by cervical dislocation. Three mice were sampled from each group for biodistribution analysis.

Sample Collection and Preparation. Blood, urine, and tissue samples were prepared as described in Simpson *et al.* with no modifications or exceptions.²⁰ Fecal samples were prepared by digestion in 500 μL of 70% Hydrochloric Acid Optima overnight, and the emulsion was diluted with ultrapure water down to 7% HCl.

Inductively Coupled Plasma–Mass Spectrometry (ICP-MS) Analysis of Biological Samples. Analysis of gold content in biological samples was performed using a Perkin-Elmer SCIEX ICP-MS (model Elan DRC-e, Vernon Hills, IL, USA) at the University of Colorado Laboratory for Environmental and Geological Sciences (LEGS). Statistical analysis of samples was performed as described in Simpson *et al.* involving the Student *t* test (95% confidence level), but with units in $\mu\text{g}/\text{mL}$.²⁰ The detection limit of the instrument was 0.02 ppb (0.02 ng Au/mL) sample.

Aggregation Study Using Relative Stomach and Intestinal pH. In order to determine if the gold nanoparticles could withstand the pH and temperature of the mouse and human gastrointestinal system (37 °C and pH as low as 2 and as high 8), samples of each gold nanoparticle formulation were tested for stability in aqueous solutions with pH ranging from 2 to 8.²⁷ This was accomplished by adjusting the pH of 20 μM solutions of gold nanoparticles to pH 2 with HCl, heating to 37 °C, and shaking for 2 h. The samples were monitored by UV–visible spectroscopy to determine the extent of aggregation. The samples were then adjusted to pH 8 to simulate conditions with the intestine and subsequently warmed to 37 °C and shaken for an additional 4 h. The results were then compared to a set of controls at pH 5 that did not undergo any pH adjustments.

Conflict of Interest: The authors declare no competing financial interest.

Acknowledgment. The authors are grateful to the Bill and Melinda Gates Foundation for many helpful discussions and generous financial support.

Supporting Information Available: Detailed particle characterization using ¹H NMR, TEM, and UV–vis is available free of charge *via* the Internet at <http://pubs.acs.org>.

REFERENCES AND NOTES

- Cutler, J. I.; Auyeung, E.; Mirkin, C. A. Spherical Nucleic Acids. *J. Am. Chem. Soc.* **2012**, *134*, 1376–1391.
- Prigodich, A. E.; Randeria, P. S.; Briley, W. E.; Kim, N. J.; Daniel, W. L.; Giljohann, D. A.; Mirkin, C. A. Multiplexed Nanoflares: mRNA Detection in Live Cells. *Anal. Chem.* **2012**, *84*, 2062–2066.
- Prigodich, A. E.; Seferos, D. S.; Massich, M. D.; Giljohann, D. A.; Lane, B. C.; Mirkin, C. A. Nano-flares for mRNA Regulation and Detection. *ACS Nano* **2009**, *3*, 2147–2152.
- Bardhan, R.; Chen, W.; Perez-Torres, C.; Bartels, M.; Huschka, R. M.; Zhao, L. L.; Morosan, E.; Pautler, R. G.; Joshi, A.; Halas, N. J. Nanoshells with Targeted Simultaneous Enhancement of Magnetic and Optical Imaging and Photothermal Therapeutic Response. *Adv. Funct. Mater.* **2009**, *19*, 3901–3909.
- Lal, S.; Clare, S. E.; Halas, N. J. Nanoshell-Enabled Photothermal Cancer Therapy: Impending Clinical Impact. *Acc. Chem. Res.* **2008**, *41*, 1842–1851.
- Lowery, A. R.; Gobin, A. M.; Day, E. S.; Halas, N. J.; West, J. L. Immunonanoshells for Targeted Photothermal Ablation of Tumor Cells. *Int. J. Nanomed.* **2006**, *1*, 149–154.
- Dickerson, E. B.; Dreaden, E. C.; Huang, X.; El-Sayed, H.; Chu, H.; Pushpanketh, S.; McDonald, J. F.; El-Sayed, M. A. Gold Nanorod Assisted Near-Infrared Plasmonic Photothermal Therapy (PPTT) of Squamous Cell Carcinoma in Mice. *Cancer Lett.* **2008**, *269*, 57–66.
- Huang, X. H.; Jain, P. K.; El-Sayed, I. H.; El-Sayed, M. A. Plasmonic Photothermal Therapy (PPTT) Using Gold Nanoparticles. *Lasers Med. Sci.* **2008**, *23*, 217–228.
- Xia, Y. N.; Li, W.; Cobley, C. M.; Chen, J.; Xia, X.; Zhang, Q.; Yang, M.; Cho, E. C.; Brown, P. K. Gold Nanocages: From Synthesis to Theranostic Applications. *Acc. Chem. Res.* **2011**, *44*, 914–924.

10. Agbasi-Porter, C.; Ryman-Rasmussen, J.; Franzen, S.; Feldheim, D. L. Transcription Inhibition Using Oligonucleotide-Modified Gold Nanoparticles. *Bioconjugate Chem.* **2006**, *17*, 1178–1183.
11. Ryan, J. A.; Overton, K. W.; Speight, M. E.; Oldenburg, C. N.; Loo, L.; Robarge, W.; Franzen, S.; Feldheim, D. L. Cellular Uptake of Gold Nanoparticles Passivated with BSA-SV40 Large T Antigen Conjugates. *Anal. Chem.* **2007**, *79*, 9150–9159.
12. Tkachenko, A. G.; Xie, H.; Coleman, D.; Glomm, W.; Ryan, J.; Anderson, M. F.; Franzen, S.; Feldheim, D. L. Multifunctional Gold Nanoparticle-Peptide Complexes for Nuclear Targeting. *J. Am. Chem. Soc.* **2003**, *125*, 4700–4701.
13. Zheng, D.; Giljohann, D. A.; Chen, D. L.; Massich, M. D.; Wang, X. Q.; Iordanov, H.; Mirkin, C. A.; Paller, A. S. Topical Delivery of siRNA-Based Spherical Nucleic Acid Nanoparticle Conjugates for Gene Regulation. *Proc. Natl. Acad. Sci. U.S.A.* **2012**, *109*, 11975–11980.
14. Bowman, M. C.; Ballard, T. E.; Ackerson, C. J.; Feldheim, D. L.; Margolis, D. M.; Melander, C. Inhibition of HIV Fusion with Multivalent Gold Nanoparticles. *J. Am. Chem. Soc.* **2008**, *130*, 6896.
15. Bresee, J.; Maier, K. E.; Boncella, A. E.; Melander, C.; Feldheim, D. L. Growth Inhibition of *Staphylococcus aureus* by Mixed Monolayer Gold Nanoparticles. *Small* **2011**, *7*, 2027–2031.
16. Bresee, J.; Maier, K. E.; Melander, C.; Feldheim, D. L. Identification of Antibiotics Using Small Molecule Variable Ligand Display on Gold Nanoparticles. *Chem. Commun.* **2010**, *46*, 7516–7518.
17. Hillyer, J. F.; Albrecht, R. M. Gastrointestinal Persorption and Tissue Distribution of Differently Sized Colloidal Gold Nanoparticles. *J. Pharm. Sci.* **2001**, *90*, 1927–1936.
18. Schleh, C.; Semmler-Behnke, M.; Lipka, J.; Wenk, A.; Hirn, S.; Schaffler, M.; Schmid, G.; Simon, U.; Kreyling, W. G. Size and Surface Charge of Gold Nanoparticles Determine Absorption across Intestinal Barriers and Accumulation in Secondary Target Organs after Oral Administration. *Nanotoxicology* **2012**, *6*, 36–46.
19. Donovan, M. D.; Flynn, G. L.; Amidon, G. L. Absorption of Polyethylene Glycols 600 through 2000: The Molecular Weight Dependence of Gastrointestinal and Nasal Absorption. *Pharm. Res.* **1990**, *7*, 863–868.
20. Simpson, C. A.; Salleng, K. J.; Cliffl, D. E.; Feldheim, D. L. *In Vivo* Toxicity, Biodistribution, and Clearance of Glutathione-Coated Gold Nanoparticles. *Nanomedicine* **2013**, *9*, 257–263.
21. Witschi, A.; Reddy, S.; Stofer, B.; Lauterburg, B. H. The Systematic Availability of Oral Glutathione. *Eur. J. Clin. Pharm.* **1992**, *43*, 667–669.
22. Simpson, C. A.; Agrawal, A. C.; Balinski, A.; Harkness, K. M.; Cliffl, D. E. Short-Chain PEG Mixed Monolayer Protected Gold Clusters Increase Clearance and Red Blood Cell Counts. *ACS Nano* **2011**, *5*, 3577–3584.
23. Jadzinsky, P. D.; Calero, G.; Ackerson, C. J.; Bushnell, D. A.; Kornberg, R. D. Structure of a Thiol Monolayer-Protected Gold Nanoparticle at 1.1 Angstrom Resolution. *Science* **2007**, *318*, 430–433.
24. Golde, W. T.; Gollobin, P.; Rodriguez, L. L. A Rapid, Simple, and Humane Method for Submandibular Bleeding of Mice Using a Lancet. *LabAnimal* **2005**, *34*, 39–43.
25. NIH guideline for animal care and use: <http://oacu.od.nih.gov/ARAC/Bleeding.pdf> (2005).
26. Kurien, B. T.; Scofield, R. H. Mouse Urine Collection Using Clear Plastic Wrap. *Lab. Anim.* **1998**, *33*, 83–86.
27. Guyton, A. C.; Hall, J. E. *Textbook of Medical Physiology*; Elsevier Saunders: Philadelphia, PA, 2006.